PS/LPI Note 85-40
April 1986

SIMULATION OF PERFORMANCE OF 30 MeV LIL-V BUNCHER

S. Kulinski, A. Riche

1. Introduction

In the preceding note [1] the process of electron bunching in the prebuncher was analysed. The most important results of this analysis were:

1) There is 100% transmission of electrons through the prebuncher even if the RF voltage V_{pB} amounts to three times the gun voltage Vg. At high level of V_{pB} some of the particles oscillate in the prebuncher field but are finally transmitted.

2) Good bunching of electrons can be obtained both for $V_{pB} \ll Vg$ and for $V_{pB} > Vg$.

3) In the case of $V_{pB} > Vg$ ($V_{pB} \approx 1.5$ to 3.0 Vg) the bunching is already realised in the prebuncher so that no drift space is necessary (see the first of figures 7 c) and prebuncher exit).

4) A rather large energy spread is produced in the case of $V_{pB} > Vg$ (figure quoted above) but the main part of bunched electrons has an energy higher than that corresponding to Vg. This indicates that most of the electrons can be accepted by the following accelerating structure which begins with rather high $\beta = 0.92$, if their phases are also appropriate.

The next question arising is what will be the buncher acceptance for both regimes of prebunching as well as what will be the energy and especially the phase spread at the end of 30 MeV buncher.

In order to answer these questions and other ones connected with amplitude and phase distortion occurring in the accelerating field in the buncher, the dynamics of electrons in the buncher have been investigated. The case of phase acceptance and phase distribution at the end of the buncher was also analysed in [2].

2. Equations of Motion

The accelerating structure of the 30 MeV LIL-V buncher is the triperiodic standing wave structure of CGR-MeV. The equations of axial motion for electrons in such structure are in principle the same as for the prebuncher and in the case of zero space charge can be written in the form

$$\frac{d\gamma}{dz} = \frac{A}{\lambda} \cos \phi$$
$$\frac{d\phi}{dz} = \frac{2\pi}{\lambda} \cdot \frac{\gamma}{\sqrt{\gamma^2 - 1}} \qquad (1)$$

The notation used here is as the same as in [1], e.g.:

$$\gamma = \frac{m}{m_0}$$

and

$$A = \frac{q\, E_z\, (z)}{m_0\, c^2} \cdot \lambda = \frac{q\, g\, (z)\, E_{zm}}{m_0\, c^2} \cdot \lambda \qquad (2)$$

where E_{zm} is the maximum of the axial component of electric field intensity in the accelerating cavity and $g(z) = E_z(z)/E_{zm}$ gives the axial variation of this field.

In principle to integrate the system of equation (1) it is necessary to know:

1) g(z)

2) the axial distribution of phase difference between neighbouring cavities. In the case of an ideal theoretical structure, this difference is π, but in the real structures as we shall see in the case of buncher V, some perturbations in the distribution can exist.

3. Measurements

In the case of the considered accelerating structure, measurements have been made allowing for a determination of at least the $E_z(z)$ distribution with some precision. In fact, two sets of measurements exist.

1) Measurements by CGR/LAL from 1980 which give g(z) and the phase distribution [3].

2) Measurements at CERN [4] (1985) of only the g(z) distribution (phase measurements were impossible since the structure was brazed and there was no access to different cavities).

It was then possible to solve the equation (1) not only for ideal but also for measured amplitude and phase distributions. To take into account the shape of accelerating field distribution in each cavity the subroutine APREZ (Approximation of E_z) was written which closely approximates the form of E_z distribution obtained by perturbation measurements. A description of this subroutine is given in Appendix I. Examples of use of this subroutine pertaining to the buncher V are presented in Figs. 1, 2, 3 and 4.

Fig. 1 presents the E_z distribution measured by CGR/LAL and Fig. 2 approximation of this distribution made by APREZ. Figs. 3 and 4 correspond to measurements made at CERN.

As it is seen from these figures the approximation seems to be good. The well visible difference in the E_z distributions obtained by CGR/LAL and at CERN are probably due to changes in the coupling cell made between these two measurements in order to improve the buncher coupling [5].

Some details given concerning the geometry of the accelerating structure of buncher V together with axial field and phase distributions are given in Table I.

The more familiar representation of E_z by functions varying by steps has also been used. We compare the results.

4. Results

1) Variation of the results with the approximation used to describe the field in the buncher.

The electric field is represented by a succession of steps or by series of third order polynomials as described in the appendix.

In Table II, the total number of transmitted electrons, from the 36 incident ones is given together with the maximum number of electrons grouped into $\Delta\phi = 10^0$ and $\Delta\phi = 20^0$ while the dephasing between the prebuncher and the buncher is varied with the aim of selecting the largest value of N_{10^0}.

The comparison of results obtained from three kinds of data:

a) theoretical amplitude, theoretical phase (quoted th, th),

b) CGR-LAL measured amplitudes and phases (LAL, LAL),

c) CERN measured amplitudes used with LAL phases (CERN, LAL)

does not show significant differences for the transmission but roughly, for approximation with step functions, we have

$$\langle E \rangle_{(LAL,\ LAL)} - \langle E \rangle_{(CERN,\ LAL)} \sim 0.7 \text{ MeV}$$

$$\langle E \rangle_{(th,\ th)} - \langle E \rangle_{(LAL,\ LAL)} \sim 1.2 \text{ MeV}$$

From the results obtained with the description by step functions and by 3rd order polynomials we conclude that the transmission, specially the value of N_{10} at optimum is about the same while the average kinetic energy is higher with the approximation by step functions, for which the size of the step has been taken equal to the length of the unit cell.

$$\langle E \rangle_{step,\ function} - \langle E \rangle_{polynomials} \sim 3.4 \text{ MeV}$$

2) Fig. 5 shows how the transmission varies with the maximum field in the prebuncher. A Gaussian shape was assumed for this field. According to R. Chaput from LAL (ref. [2]), the relation between the tension and the maximum field in the cavity is given by $E_0 = V_0/\sqrt{2\pi}\ \ \sigma$, with $\sigma = 7.11$ mm. The results are plotted for the value of the dephasing between prebuncher and buncher which gives the maximum for N_{10°.

This dephasing is represented in c), while N_{10}/N_{360} transmitted is given in b).

The corresponding total transmission, given in a), is very similar to the one given by R. Chaput and displayed in Fig. 6.

Fig. 5 is a summary of the data of Table III in which values are given according to 3 different optimisations, i.e. of total transmission N_{360°, of N_{10°, of N_{20°. There is a large difference for N_{10° depending on what is optimized: total transmission or N_{10°, but only for prebuncher field $E_0 > 2.7$ MVm^{-1}.

3) Fig. 7 shows energy-phase diagrams for the particles at prebuncher exit, buncher entry and exit, for 3 values of the prebuncher central field.

   a) with a low central field of 1.2 MV m^{-1}, the beam is only slightly modulated in energy at prebuncher exit. This gives already some bunching in phase at buncher entry. Strong bunching is achieved by the buncher . At 7.5 MV m^{-1} and 12 MV m^{-1}, the modulation in energy is important at prebuncher exit. The shift between prebuncher and buncher does not contribute to the bunchig in phase, while the buncher effect is strong. The high voltage prebunching introduces more dispersion in energy than the low one.

4) Fig. 8 shows corresponding phase and energy histograms, as projection of preceding figures onto their axis. From the point of view of energy dispersion low field prebunching seems to be preferable. On the other hand, as shown on Fig. 5b) and c), a large variation of the number of particles transmitted into 10° can happen for small field and phase changes. High field bunching appears to be more favorable from the stability point of view.

There is a good agreement between our results and those of R. Chaput as far as the total transmission is concerned. It is also interesting to note that for high field bunching, there are usually 2 peaks in energy distribution, which also agree very well with the measurements made at LAL [6].

ACKNOWLEDGEMENTS

We would like to express our thanks to K. Hübner who constantly supported our work with suggestions and remarks.

REFERENCES

1) S. Kulinski, Large signal electron bunching, PS/LPI/Note/85-11

2) R. Chaput, Fonctionnement de la cavité de prégroupement CGR-MeV à fort champ, LAL PI 85-20/T

3) J.C. Bourdon et J. Rodier, Compte rendu des mesures HF sur le groupeur de la station d'essai, LAL/PI 80-87

4) A. Bellanger, S. Kulinski and D.J. Warner, RF Measurements on the LIL-V buncher at CERN, PS/LPI/Note 85-10

5) J.C. Bourdon, J. Rodier, Compte rendu sur le groupeur de la station d'essai, LAL/PI/80-87

6) R. Belbéoch, Longueur des paquets d'électrons à la sortie du groupeur du linac préinjecteur du LEP, LAL PI 85-18 T.

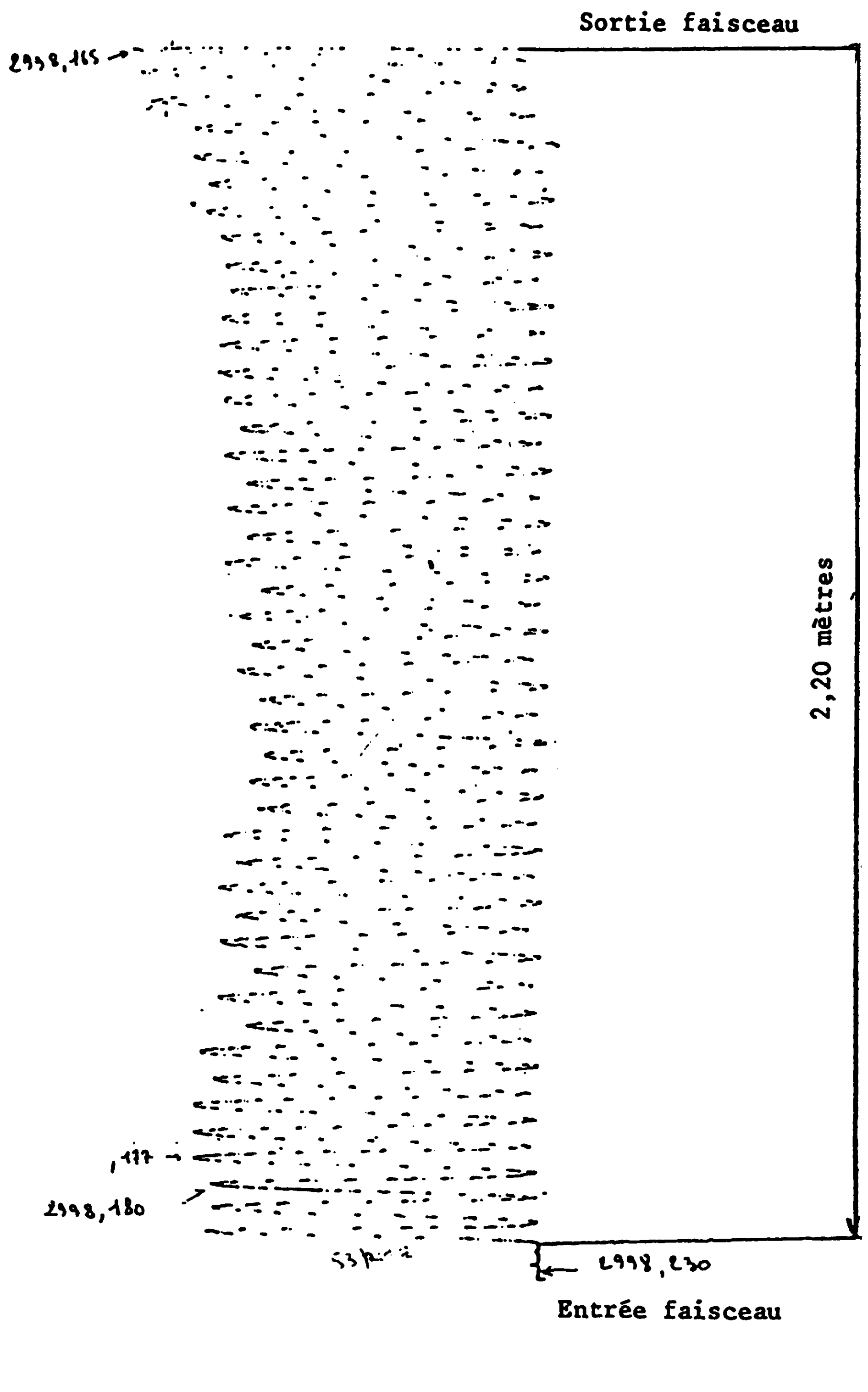

Fig. 1 - BUNCHER V

$\Delta f \sim E_z^2$ DISTRIBUTION ALONG THE AXIS - MEASUREMENTS LAL

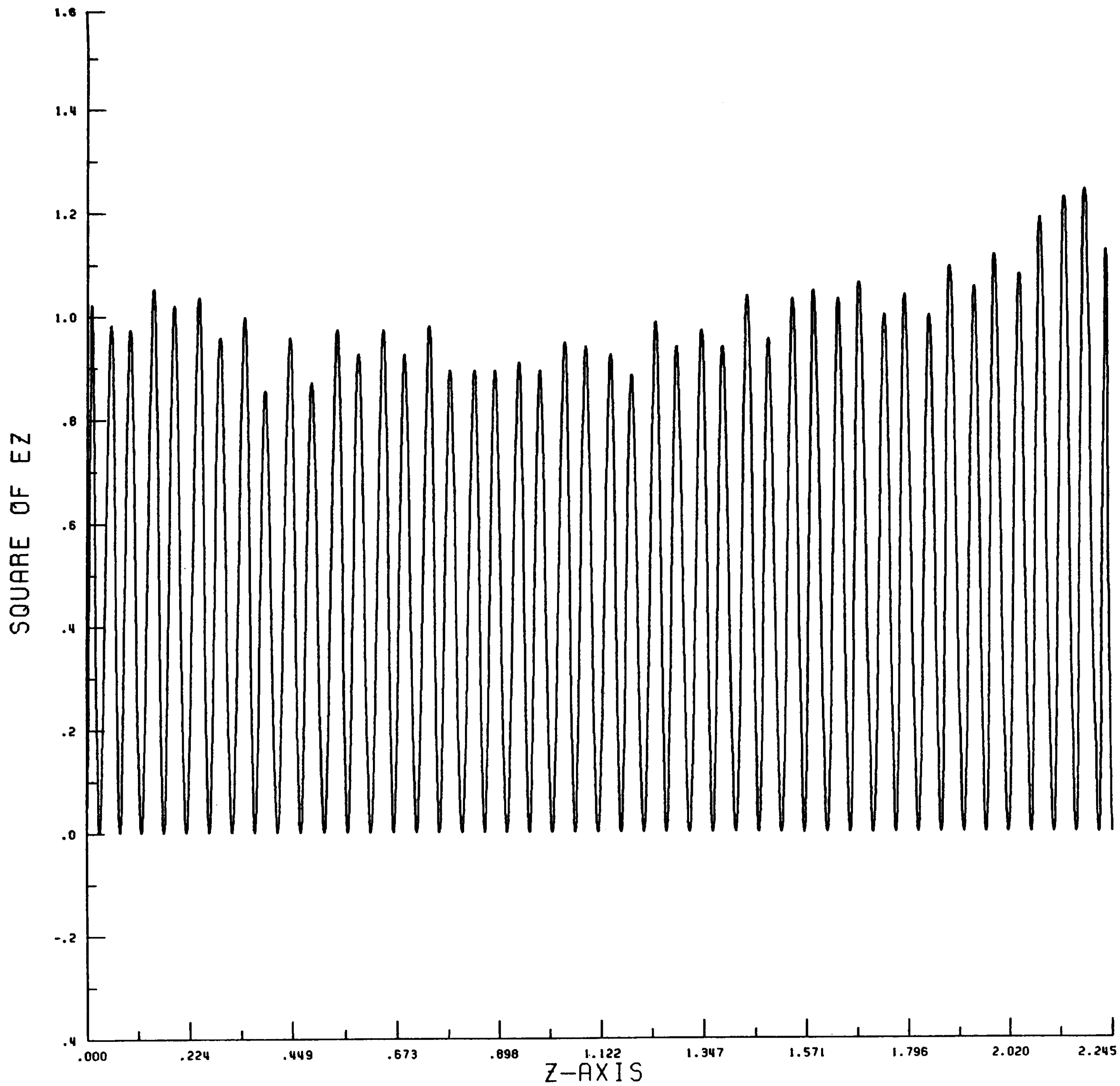

Fig. 2 - BUNCHER V

CGR-LAL MEASUREMENTS APPROXIMATED ACCORDING TO "APREZ"

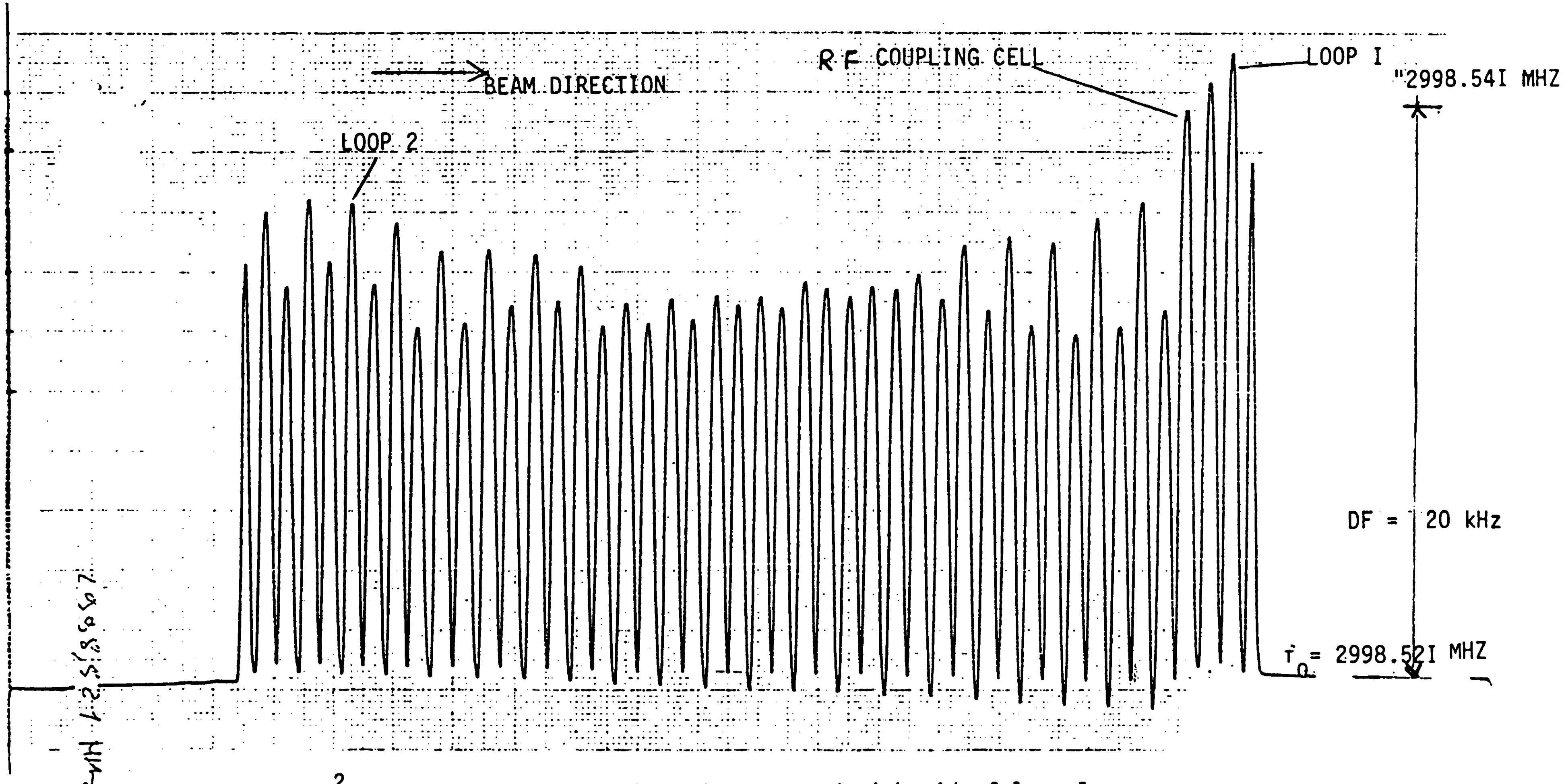

~~FIG. 10~~ $\Delta f \sim E_z^2$ distribution along the axis measured with aid of loop I

Fig. 3 - BUNCHER V - MEASUREMENTS CERN

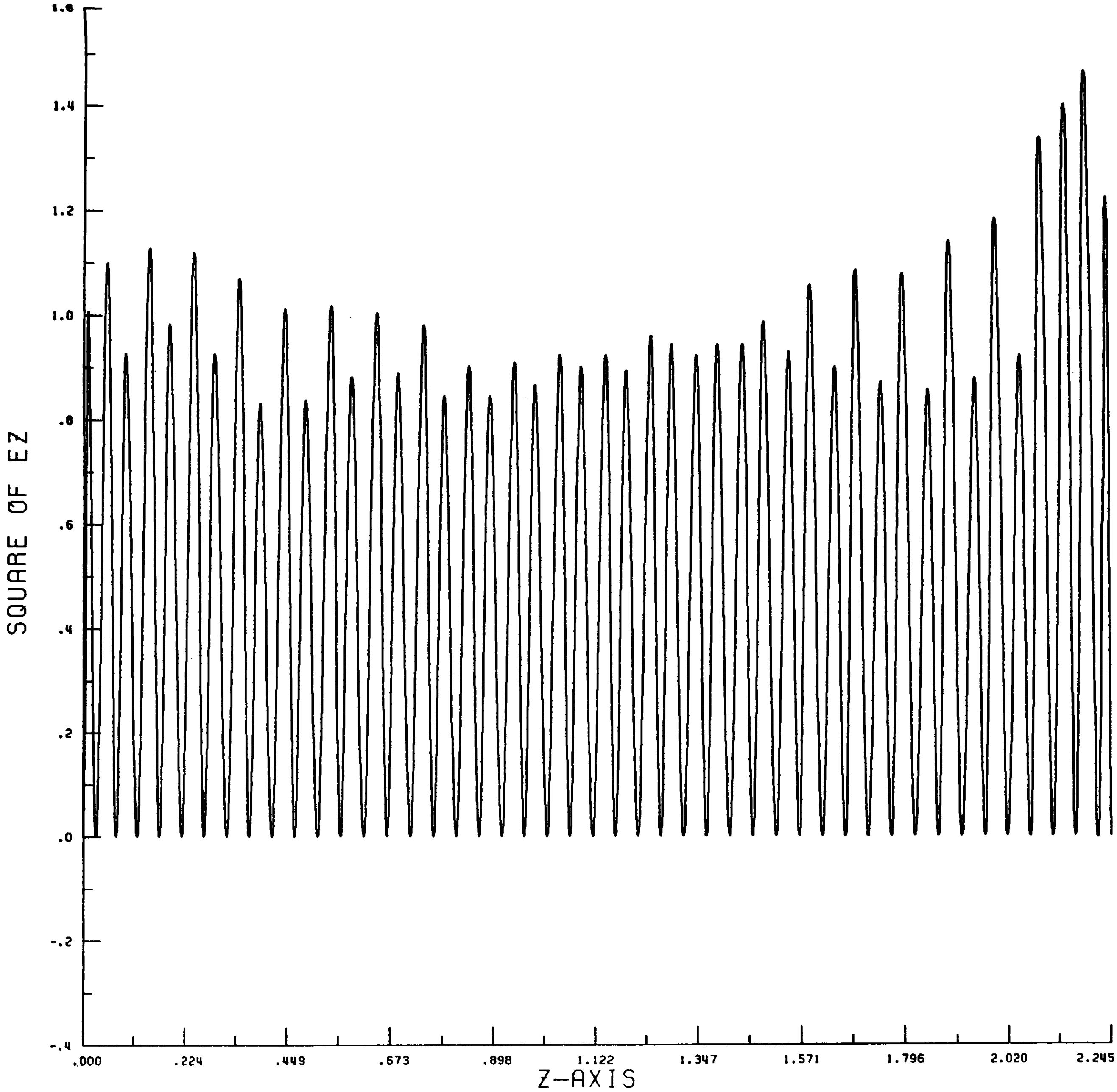

Fig. 4 - BUNCHER V

CERN MEASUREMENTS APPROXIMATED ACCORDING TO "APREZ"

Fig. 5

MAXIMUM TRANSMISSION AND MAXIMUM TRANSMISSION IN ΔPHASE = 10°

THE DEPHASING BUNCHER - PREBUNCHER IS OPTIMISED FOR TRANSMISSION IN 10°

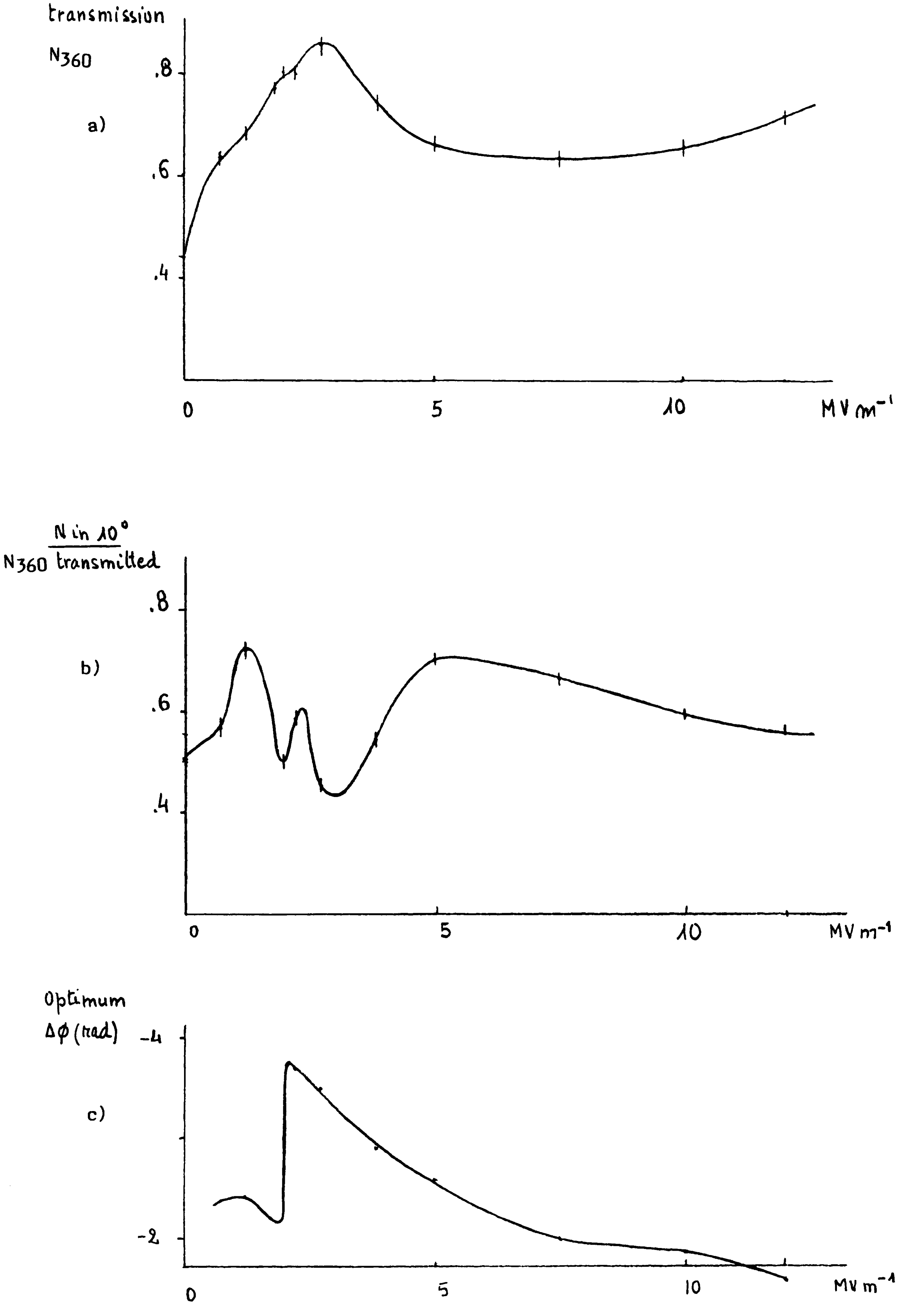

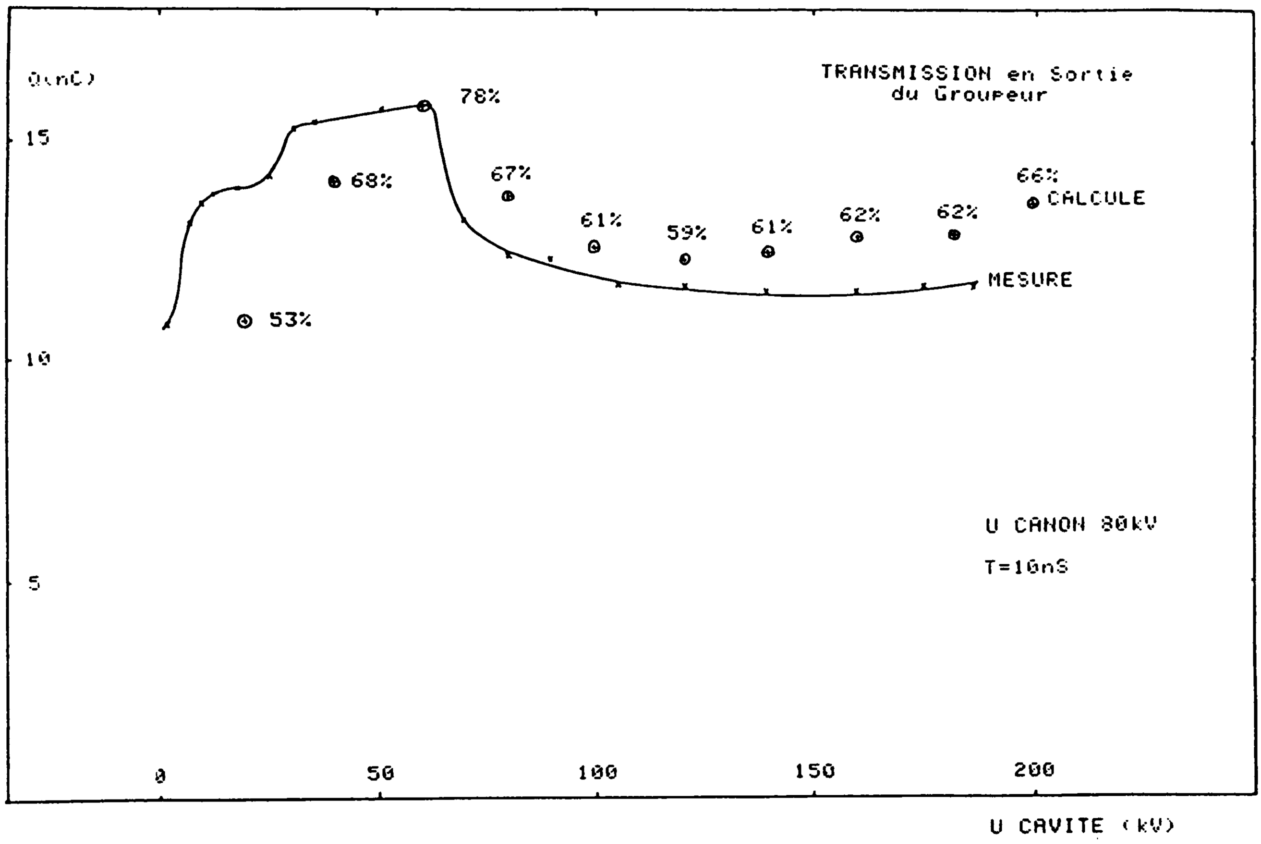

Q(nC)
TRANSMISSION en Sortie du Groupeur
15
10
5
78%
68%
67%
66%
CALCULE
61%
59%
61%
62%
62%
MESURE
53%
U CANON 80kV
T=10nS
0
50
100
150
200
U CAVITE (kV)

Fig. 6

Fig. 7 a) E prebuncher 1.2 MV m^{-1} (21.5 kV) phase (prebuncher - buncher) optimised

at prebuncher exit | at buncher entry | at buncher exit

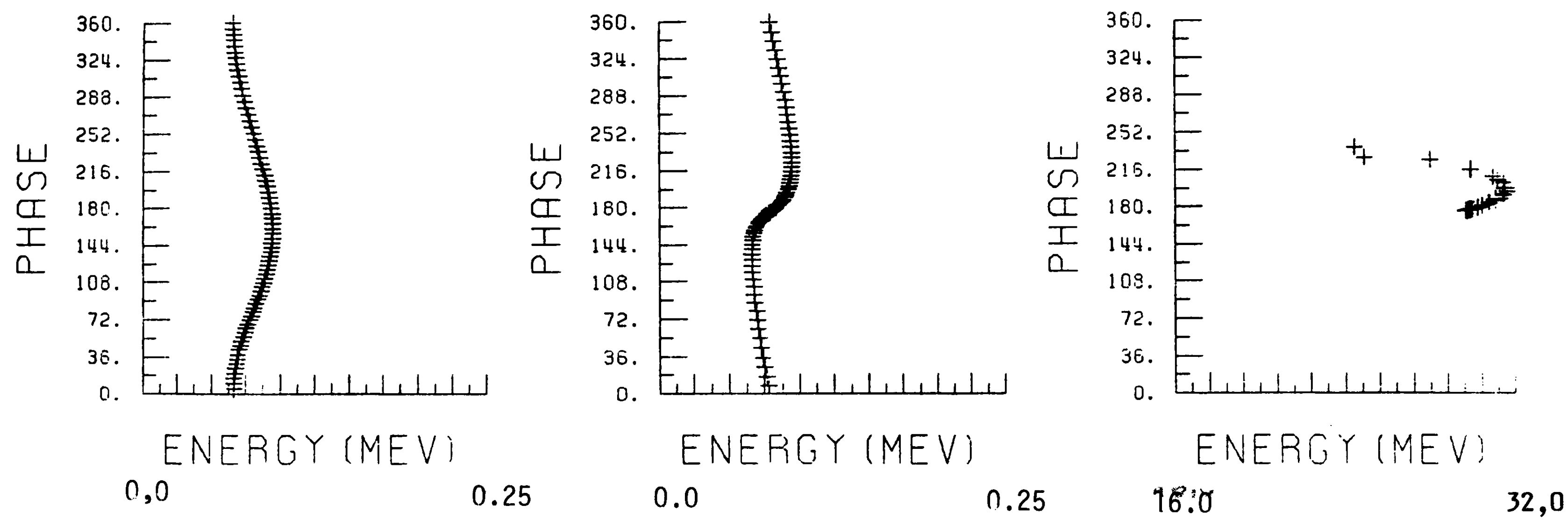

b) $\hat{E}$ prebuncher 7.2 MV m^{-1} (136 kV)

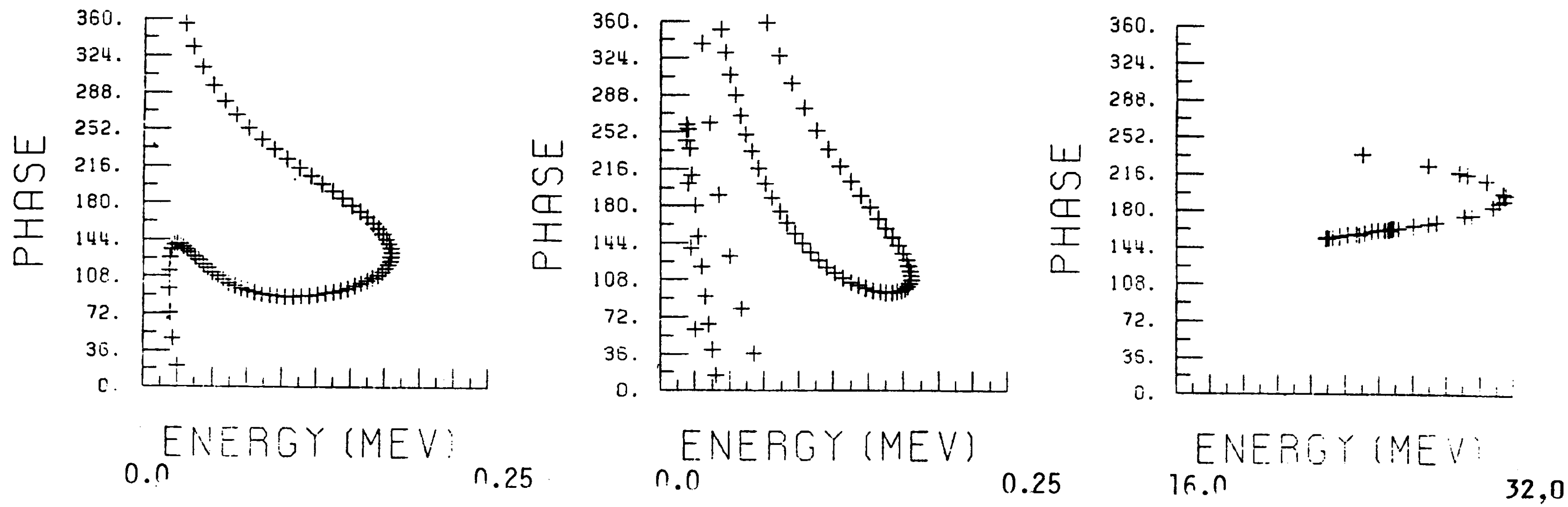

c) $\hat{E}$ prebuncher 12 MV m^{-1} (214.6 kV) phase prebuncher - buncher optimised

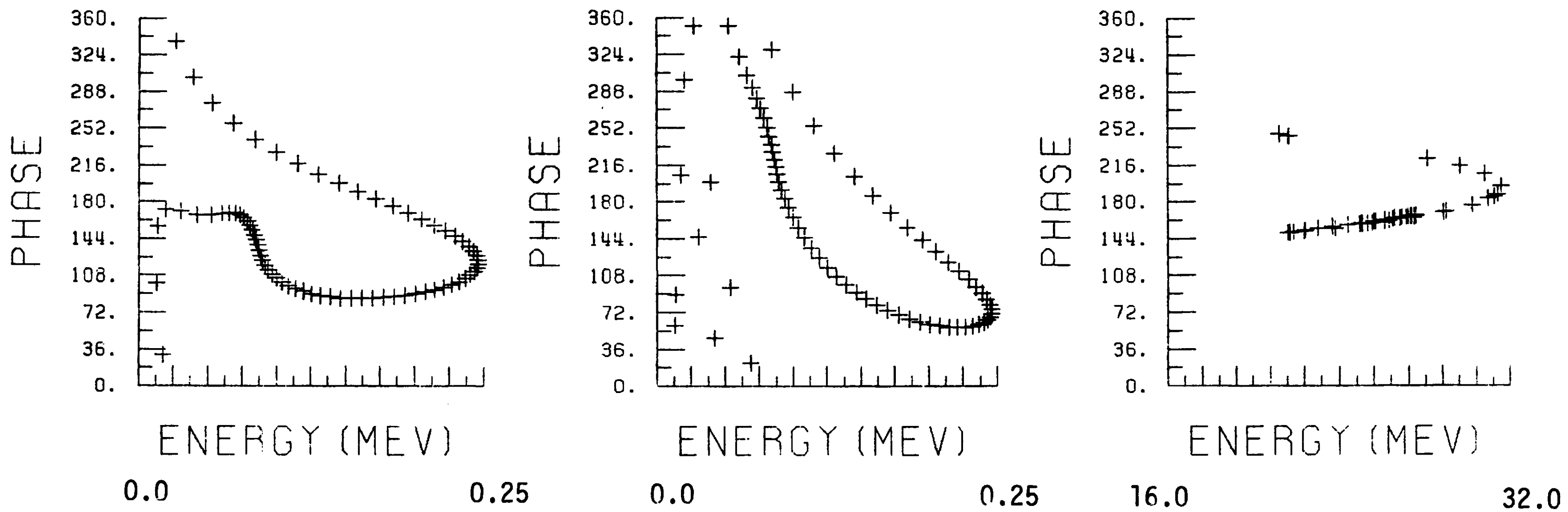

Fig. 8

Prebuncher $\hat{E}$ 1.2 MV m^{-1} (21.5 kV)

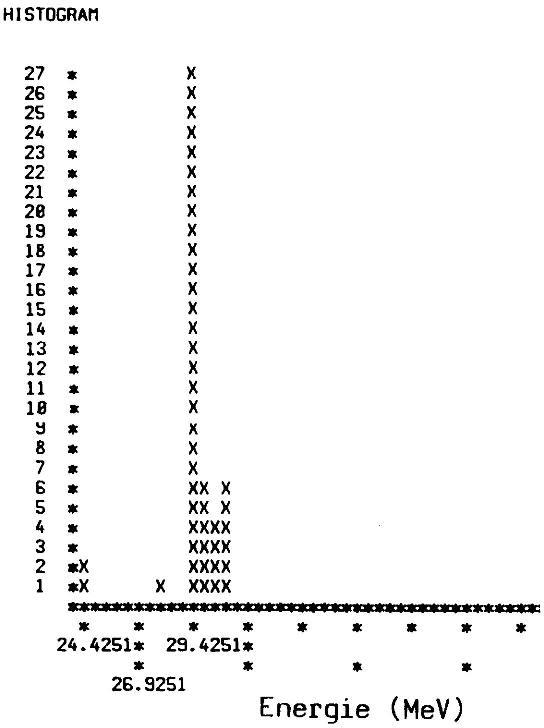

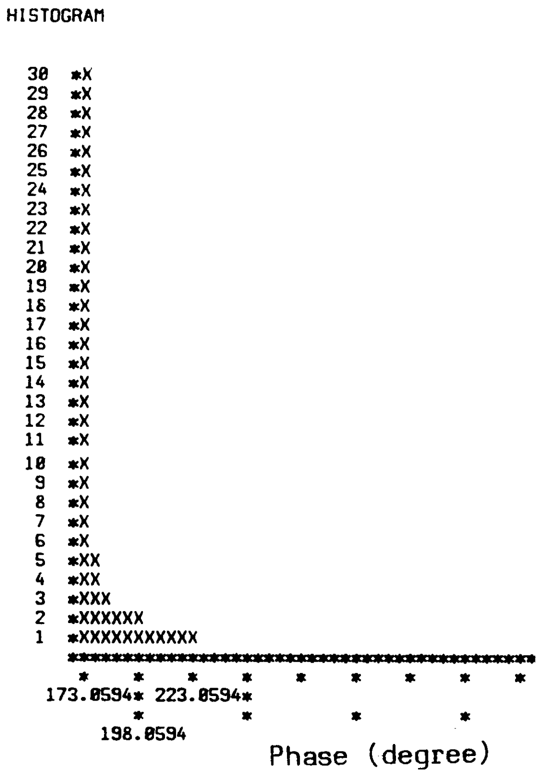

Prebuncher $\hat{E}$ 7.5 MV m^{-1} (136 kV)

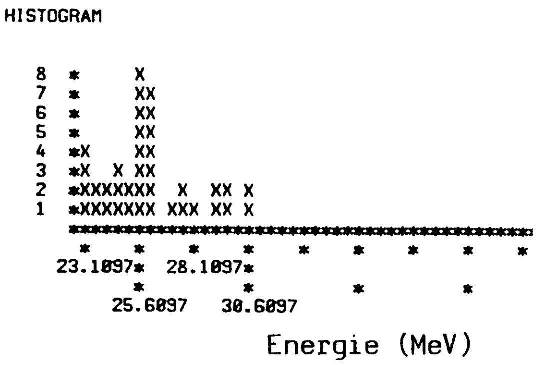

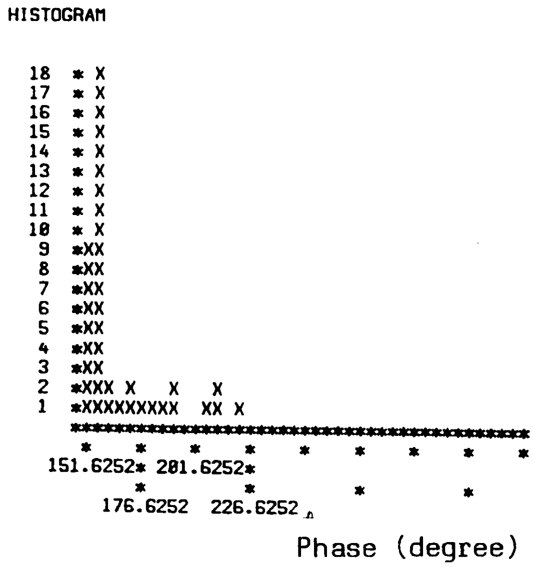

Prebuncher $\hat{E}$ 12 MV m^{-1} (214.6 kV)

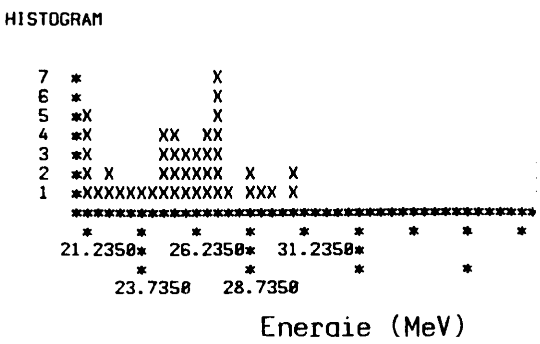

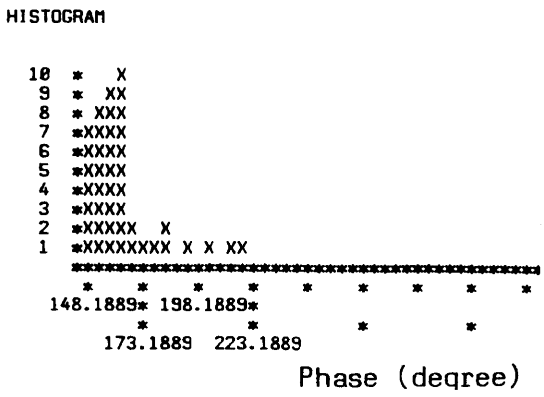

TABLE I

GEOMETRICAL AND ELECTRICAL DATA FOR 3rd POLYNOMIAL APPROXIMATION OF E_z^2

CELL NB	ZO(I)	ZM(I)	EZ2/<EZ2> MEAS.CERN	THEORET. D-PHASE	EXPERIMENTAL D-PHASE	EZ2/<EZ2> MEAS.CGR LAL
1	.000	.0085	1.007	-PI	-3.1415927	1.0220
2	.027	.0525	1.100	+PI	3.2044245	.9827
3	.073	.0935	.928	-PI	-3.2131512	.9749
4	.119	.1460	1.129	+PI	3.2236231	1.0535
5	.168	.1900	.985	-PI	-3.2410764	1.0220
6	.217	.2445	1.122	+PI	3.2672564	1.0378
7	.267	.2895	.928	-PI	-3.2672564	.9592
8	.317	.3445	1.072	+PI	3.2672564	.9985
9	.367	.3895	.834	-PI	-3.2306044	.8570
10	.417	.4445	1.014	+PI	3.2567844	.9592
11	.467	.4895	.841	-PI	-3.3143803	.8727
12	.517	.5445	1.021	+PI	3.2934363	.9749
13	.567	.5895	.885	-PI	-3.3457962	.9277
14	.617	.6445	1.007	+PI	3.2829643	.9749
15	.667	.6895	.892	-PI	-3.3772121	.9277
16	.717	.7445	.985	+PI	3.2485222	.9827
17	.767	.7895	.849	-PI	-3.3719761	.8963
18	.817	.8445	.906	+PI	3.3457962	.8963
19	.867	.8895	.849	-PI	-3.4086280	.8963
20	.917	.9445	.913	+PI	3.3772121	.9120
21	.967	.9895	.870	-PI	-3.4400440	.8963
22	1.017	1.0445	.928	+PI	3.3876841	.9513
23	1.067	1.0895	.906	-PI	-3.4505159	.9434
24	1.117	1.1445	.928	+PI	3.4348080	.9277
25	1.167	1.1895	.899	-PI	-3.4609879	.8884
26	1.217	1.2445	.964	+PI	3.4505159	.9906
27	1.267	1.2895	.949	-PI	-3.5133478	.9434
28	1.317	1.3445	.928	+PI	3.4976398	.9749
29	1.367	1.3895	.949	-PI	-3.4505159	.9434
30	1.417	1.4445	.949	+PI	3.4871678	1.0419
31	1.467	1.4895	.993	-PI	-3.5866516	.9592
32	1.517	1.5445	.935	+PI	3.5116025	1.0378
33	1.567	1.5895	1.064	-PI	-3.5953783	1.0535
34	1.617	1.6445	.906	+PI	3.5814156	1.0378
35	1.667	1.6895	1.093	-PI	-3.6075956	1.0692
36	1.717	1.7445	.877	+PI	3.6023596	1.0063
37	1.767	1.7895	1.086	-PI	-3.6494835	1.0456
38	1.817	1.8445	.863	+PI	3.6180675	1.0063
39	1.867	1.8895	1.151	-PI	-3.6547195	1.1007
40	1.917	1.9445	.885	+PI	3.6390115	1.0614
41	1.967	1.9895	1.194	-PI	-3.5290557	1.1243
42	2.017	2.0445	.928	+PI	3.5866516	1.0849
43	2.067	2.0895	1.352	-PI	-3.0735248	1.1950
44	2.117	2.1445	1.417	+PI	3.0682888	1.2343
45	2.167	2.1895	1.482	-PI	-3.1206487	1.2500
46	2.217	2.2358	1.237	+PI	3.1415927	1.1321

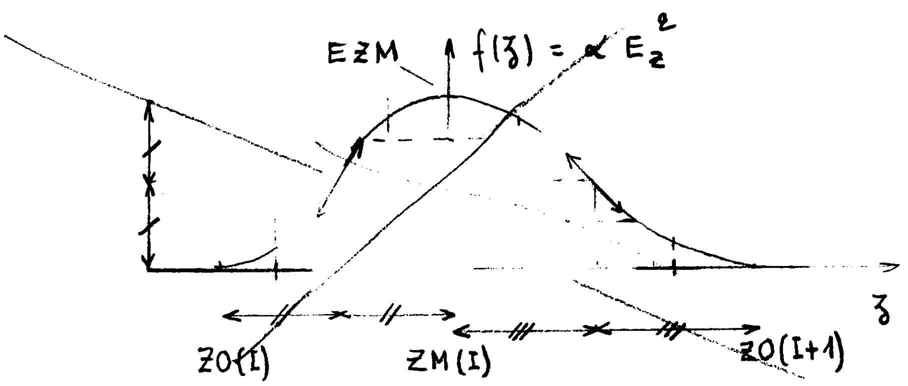

TABLE II

COMPARISON OF RESULTS FROM VARIOUS APPROXIMATED DATA

$\hat{E}$ prebuncher = 7.5 MV m^{-1}

1. Approximation of the Function E_z by Steps

$E_{(z)}$	Phase	ΔØ near optimisation (rad)	N_{36}	N_{10}	N_{20}	kinetic energy (average)
theoretical	theoretical	-1.8	20	13	14	27.99
		-1.9	20	13	15	27.94
		-2.0	20	13	15	28.08
		-2.1	22	13	16	27.62
		-2.2	22	12	16	28.10
		-2.3	22	11	17	28.46
measurements LAL	measurements LAL	-1.8	21	13	14	26.38
		-1.9	20	13	15	26.77
		-2.0	20	13	15	26.77
		-2.1	22	13	16	26.70
		-2.2	22	12	16	27.17
		-2.3	22	11	16	27.54
measurements LAL	measurements LAL	-1.8	21	13	14	25.72
		-1.9	20	13	15	25.91
		-2.0	22	13	15	26.65
		-2.1	22	13	16	26.06
		-2.2	22	12	16	26.49
		-2.3	22	11	16	26.83

2. Approximation of the Function E_z^2 by third order Polynomials

E_z^2	phase	ΔØ	N_{36}	N_{10}	N_{20}	< E >
theoretical	theoretical	-3.7	20	13	14	24.74
		-3.8	22	13	15	24.43
measurements LAL	measurements LAL	-3.4	22	11	15	23.40
		-3.5	20	12	14	23.50
		-3.6	21	12	14	23.33
		[-3.7	22	13	14	23.40
		[-3.8	23	13	14	23.45
		-3.9	22	12	17	23.70
		-4.0	23	12	17	23.74
		-4.2	23	8	16	24.07
measurements CERN	theoretical	-3.7	20	13	14	24.72
		-3.8	22	13	15	24.44

TABLE III

INFLUENCE OF PRE-BUNCHER MAXIMUM CENTRAL FIELD UPON TRANSMISSION AND OPTIMUM BUNCHING

Statistics obtained with 36 particles with uniform initial distribution in phase (General phase origin arbitrary)

Data: measured amplitudes and phases at CGR-LAL

$\hat{E}$ max Prebuncher (MVm^{-1})	For maximum total transmission: Transmission Max total N_{36}	Transmission in 10° N_{10}	Transmission in 20° N_{20}	Phase (rad)	Maximum transmission in $\Delta\phi = 10^{\circ}$: Transmission Total N_{36}	Max in 10° N_{10}	in 20° N_{20}	Phase (rad)	Maximum transmission in $\Delta\phi = 20^{\circ}$: Transmission Total N_{36}	in 10° N_{10}	Max. in 20° N_{20}	Phase (rad)
0	16	8	10									
0.7	23	13	16	- 2.4	23	13	16	- 2.4	23	13	16	- 2.4
1.2	25	18	20	- 2.4	25	18	20	- 2.4	25	18	20	- 2.4
1.7	28	14	23	- 2.4	27	16	23	- 2.2	27	16	23	- 2.2
1.925	29	14	22	- 3.0	29	14	22	- 3.0	29	12	23	- 2.6
2.2	29	17		- 3.7	29	17		- 2.7				
2.7	31	14	21	- 3.5	31	14	21	- 3.5	31	14	21	- 3.5
3.8	27	8	14	- 3.5	26	14	16	- 2.9	26	13	18	- 3.2
5.0	24	12	17	- 2.8	20	14	16	- 2.6	24	12	17	- 2.8
7.5	23	9	15	- 2.5	20	13	15	- 2.0	22	12	16	- 2.2
10.0	24	9	14	- 2.3	22	13	17	- 1.9	22	13	17	- 1.9
12.0	26	8	12	- 2.2	23	13	17	- 1.6	23	10	18	- 1.7